ChemCatChem

The European Society Journal for Catalysis

Chemistry Europe

European Chemical Societies Publishing

Supported by

GeCatS

GERMAN CATALYSIS SOCIETY

Accepted Article

WILEY-VCH

Co-immobilization and colocalization of multi-enzyme systems for the cell-free biosynthesis of aminoalcohols

Susana Velasco-Lozano,[a] Javier Santiago-Arcos,[b] José A. Mayoral,[a] and Fernando López-Gallego.*[b,c]

[a]   Prof. José Antonio Mayoral, Dr. Susana Velasco Lozano
        Catálisis Heterogénea en Síntesis Orgánicas Selectivas
        Instituto de Sïntesis Química y Catálisis Homogénea (ISQCH-CSIC), University of Zaragoza
        Pedro Cerbuna, 12, 50009, Zaragoza, Spain
[b]   Prof, Fernando, López Gallego* and Javier Santiago Arcos
        Heterogeneous biocatalysis laboratory.
        Center for Cooperative Research in Biomaterials (CIC biomaGUNE), Basque Research and Technology Alliance (BRTA),
        Paseo de Miramon 194, 20014, Donostia San Sebastián, Spain
        E-mail: flopez@cicbiomagune.es
[c]   Prof. Fernando López Gallego
        IKERBASQUE, Basque Foundation for Science
        Maria Diaz de Haro 3, 48013 Bilbao, Spain

        Supporting information for this article is given via a link at the end of the document WWW under http://dx.doi.org.

Abstract: The manufacturing of aminoalcohols is an appealing transformation for industrial biocatalysis due to their high value as building blocks in synthetic chemistry. By co-immobilizing dehydrogenases, ω-transaminases and oxidases on porous carriers, we fabricated and characterized a multi-functional heterogeneous biocatalyst that was further applied to the cell-free biosynthesis of amines and aminoalcohols from alcohols and diols, respectively. This immobilized cascade integrates both redox cofactor and amine donor recycling systems into the amino alcohol biosynthesis. Spatial co-localization of the multi-enzyme system significantly increases the cofactor recycling efficiency, the system productivity and the product conversion. Using this multi-functional heterogeneous biocatalyst, we achieved 80% conversion of alcohols into amines and accessed a palette of up to 5 aminoalcohols starting from their corresponding diols in one-pot. The results herein presented contribute to understanding the effects of the confinement of co-immobilized enzymes on the cascade processes.

Introduction

The direct conversion of alcohols into amines is a valuable chemical transformation in synthetic chemistry since the latter are key useful chemical intermediates for the production of industrially relevant bioactive compounds.[1] In particular, chemical routes towards aminoalcohols underpin the synthesis of many drugs both already marketed but also in development.[2] Yet their chemical synthesis is cumbersome and poorly sustainable due to its limited chemo and regioselectivity, high reaction temperatures and complex work-up.[3] Alternatively, biocatalytic approaches offer rather selective synthetic methods

under milder conditions, which ease the downstream processes to access enantiopure products. Furthermore, biocatalysts are ideal to drive step-wise synthesis in one-pot without separation and purification steps, decreasing the generated wastes. Besides, enzyme cascades also minimize intermediate inhibition, shift the equilibrium towards the target products, and recycle the pool of cofactors. All in all increases the overall catalytic efficiency and sustainability of the process.[4] [5]

Whole-cell biotransformations and cell-free soluble systems have been optimized to synthesize aminoalcohols from different starting materials[6] such as aldoses,[7] epoxides,[8] aminoacids and aldehydes.[9] Manufacturing aminoalcohols from bio-based diols advances the concept of biorefinery, broadening the synthetic toolbox to transform bio-based raw materials into high-added value chemicals.[10] In this context, the most exploited biocatalytic system to convert diols into amino alcohols or diamines, relies on sequentially coupling alcohol dehydrogenases (ADH) and ω-transaminases (ωTA) connected with an L-alanine dehydrogenase (L-AlaDH) that orthogonally recycles redox cofactor and amine donor, shifting the amination equilibrium at the expense of ammonia (Scheme 1). Resting cells harboring an artificial operon that encodes these three enzymes failed to produce pure aminoalcohols in one-pot as the cascade continued the oxidation/amination sequence until reaching the corresponding diamine.[6] As alternative to whole-cell biotransformations, cell-free systems have also been exploited for the synthesis of amino alcohols.[11] Soluble ADH, ωTA and L-AlaDH perform the bioamination of primary alcohols in a redox self-sufficient system.[12] When diols were utilized as

substrate, 1,ω-amino alcohols were prepared but mixed with 1,ω-diamines since two consecutive redox-neutral oxidation-amination sequences partially occurred. Similar to what occurs with whole-cell biotransformation, halting the enzyme cascade in the amino alcohols is rather challenging even using isolated enzymes.

When using cell-free multi-enzyme cascades, the isolation and purification of enzymes result in less robust and sometimes inefficient catalytic processes due to the lack of a chassis that protect the enzymes and confine them. Moreover, purification costs may limit the economic feasibility of the process. To overcome these drawbacks, selective immobilization of enzymes emerges to simultaneously purify and heterogenize cell-free multi-enzymatic systems from crude extracts.[13] This pure and immobilized enzymes turn out to be operationally stable and reusable, beside their capacity to be easily separated from the reactants once the reaction is completed.[14] Furthermore, immobilized enzyme systems are gaining momentum in flow biocatalysis, leading to more sustainable and robust processes [5e, 15].

Immobilization also promotes an enzyme confinement that may resemble the crowded environment of native enzymatic cascades within living cells. Metabolic pathways in living cells are normally confined into the same micrometric space and perfectly orchestrated to enhance the chemical fluxes towards the target product. In fact, the spatial organization and the confinement of multi-enzyme systems into solid materials is drawing the attention of the biocatalysis community. It has been observed that the position of enzymes across the structures of the carriers affect the performance of the heterogeneous biocatalytic system.[16] Therefore, controlling the position of cell-free enzyme systems into solid materials, one may mimic the spatial organization found in native biosynthetic pathways and even create artificial ones .[5b] Nevertheless, preserving high activity and stability of all the enzymes upon the immobilization is an arduous task.[17] Despite these challenges, the development of new multi-enzyme systems selectively co-immobilized is increasingly driven by economic and environmental constraints that provide an incentive to develop alternatives to conventional multistep synthetic methods.[18]

In this work we describe the fabrication of a multi-functional heterogeneous biocatalyst for the one-pot synthesis of amino alcohols starting from renewable diols. The biocatalyst comprises a co-immobilized redox-neutral enzymatic cascade composed of 2 main enzymes working in tandem; an ADH and a ωTA, and one auxiliary enzyme; L-AlaDH (Scheme 1). The site-selective and classical immobilization protocol based on His-tagged enzymes opens a new optimization window to control their space localization aiming at enhancing the aminoalcohol production. Besides, cofactor recycling and equilibrium shifting were decoupled by co-immobilizing a fourth enzyme; a NADH oxidase that replenishes the NAD$^+$ pool using molecular oxygen as electron acceptor. These multi-functional heterogeneous biocatalysts were challenged for the synthesis of 1 model aromatic amine and 6 different amino alcohols - including both aromatic and aliphatic ones - from 1 aromatic alcohol and 6 different diols, respectively.
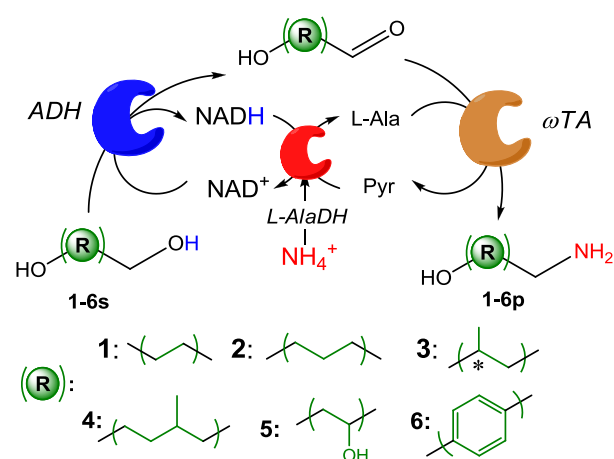
Scheme 1. One-pot multi-enzymatic synthesis of aminoalcohols by redox-neutral amination of diols. ADH: Alcohol dehydrogenase. ωTA: ω-transaminase. L-AlaDH: L-alanine dehydrogenase. L-Ala: L-alanine. Pyr: Pyruvate: 1) 1,3-propanediol. 2) 1,4-butanediol. 3) 3-hydroxy-1-butanol. 4) 3-methyl-1,5-pentanediol. 5) glycerol. 6) *p*-hydroxy benzyl alcohol.

Results and Discussion

The one-pot redox-neutral biotransformation of diols into amino alcohols requires the smart orchestration of three enzymes; ADH, ωTA and L-AlaDH (Scheme 1). This cascade starts with the ADH-driven oxidation of one of the terminal hydroxyl groups from the starting diol, producing the corresponding hydroxy aldehyde, and concomitantly reducing stoichiometric amounts of the NAD$^+$ cofactor. Then, the resulting hydroxy aldehyde is concurrently aminated through a transamination reaction catalyzed by ωTA that yields the desired aminoalcohol using L-alanine (L-Ala) as amine donor. Both oxidation and transamination steps are reversible as the accumulation of both the reduced cofactor (NADH) and pyruvate (Pyr) reverts the equilibrium towards the reduction and deamination reactions, respectively. In order to shift both equilibria, NAD$^+$ must be *in*

2

situ recycled to assure that the cofactor pool remains in its oxidized form,[19] and a large excess of amine donor (up to 50-fold) is required to shift the equilibrium towards the amination reaction.[20] To that aim, L-AlaDH simultaneously replenishes the NAD$^+$ pool and shifts the equilibrium towards the amination reaction through catalyzing a NADH-dependent reductive amination that converts Pyr back into L-Ala at the expense of ammonia as primary amine source[6, 12, 21] (Scheme 1). Unfortunately, this pathway has been only explored for 1,ω-diols with limited yields for aminoalcohols due to the over oxidation/amination of the two hydroxyl groups, which also yields the corresponding 1,ω-diamines.[12, 21b]

In this work, we started reproducing the redox-neutral multi-enzyme system already described by Kroutil group,[12] just through mixing crude extracts of ADH from *Bacillus stearothermophilus* (BsADH),[22] *L*-AlaDH from *Bacillus subtilis* (BsAlaDH)[23] and one S-selective ωTA. We screened two different ωTAs: the one from *Chromobacterium violaceum* (CvωTA)[24] already exploited for the synthesis of amino alcohols, and the less common ωTA from *Pseudomonas fluorescens* (PfωTA)[25] that is currently investigated in our laboratory.[26] Initially, we tested the soluble system for the oxidation/amination cascade of a model alcohol; benzyl alcohol, to yield benzylamine. Herein, we studied the enzyme activity ratio to maximize both overall rate and yield for aminoalcohol synthesis (Table 1).

We starting using CvωTA as transaminase since it was proven to work out for this cascade.[12] The activity ratio 1:6:10 (ADH: ωTA:L-AlaDH) was found to be roughly 2-fold more efficient than the ratio 1:1:10, which indicates that excesses of both ωTA and L-AlaDH are needed to guarantee the NAD$^+$ recycling and the equilibrium shift towards the amination reaction. Interestingly, these three enzymes fully interplay, which makes that the NAD$^+$ pool is only replenished if the ωTA performs the transamination reaction. When higher activity ratios (1:19:33) were intended at the cost of decreasing the ADH activity, both yield and overall rate (conversion lower than 30%) decreased, but the specific system productivity regarding the amount of ADH significantly increased by 3-fold factor. We also tested different amino donors for the direct amination of benzaldehyde. *L*-alanine showed the best result compared with *L*-serine, isopropylamine, polyethyleneimine, poly-*L*-lysine and polyallylamine (Table S1). This result establishes the L-AlaDH/L-Ala as the best pair to simultaneously recycle the cofactor and shift the equilibrium towards the aminated products. Hereinafter, we set the enzyme

ratio at 1:6:10 (ADH: ωTA:L-AlaDH) and L-Ala as amino donor for further experiments.

Table 1. Effect of enzyme ratio in the performance of the multi-enzymatic system synthesizing benzylamine starting from benzyl alcohol

Activity ratio ADH: ωTA:L-AlaDH	Rate (μM/min)	SSP[c] (μM/min x mg$_{BsADH}$)	Benzylamine yield (%)
1:1:10[a]	6.6	22	12
1:3:10[a]	7.3	24	21
1:6:10[a]	11.8	39	28
1:19:33[b]	9.9	110	21

All reactions were carried out in plastic tubes where cell lysate extracts were placed and mixed at a final volume of 1.5 mL with a reaction mixture consisted of 50 mM of benzyl alcohol at pH 8.5 with NAD$^+$ 0.75 mM, PLP 0.35 mM, L-Alanine 250 mM, NH$_4$Cl 275 mM and DMSO 10%; incubated at 40 rpm at 25ºC. Conversions were measured after 20 h of reaction. [a] ADH activity in reaction = 0.2 U (0.30 mg of BsADH). [b] ADH activity in reaction = 0.06 U (0.09 mg of BsADH). [c] SSP: Specific system productivity defined as the rate divided by the mass amount of BsADH in the reaction.

Immobilization and characterization of different heterogeneous biocatalysts.

Since our goal is heterogenizing the multi-enzyme system for manufacturing amino alcohols from diols, the three enzymes were either separately immobilized on 3 different carriers (HB3-3) or co-immobilized on the same carrier (HB3-1) at the optimal enzyme ratio aforementioned. We chose cobalt-activated agarose microbeads (AG-Co^{2+}) as a suitable carrier for the one-step purification and immobilization of the three His-tagged enzymes. Using this immobilization chemistry, enzymes are reversibly, but strongly, attached to the carrier, trough metal coordination bonds selectively formed between the cobalt-chelates on the agarose surface and the histidines fused at the N-*terminus* of the enzymes. SDS-PAGE (Figure S1) demonstrates that each enzyme was selectively immobilized. This immobilization methodology is widely exploited in biocatalysis,[25, 27] since it allows us directly using crude extracts for the preparation of the heterogeneous biocatalysts, thus reducing preparative steps.

Table 2 shows the immobilization parameters of both separately immobilized and co-immobilized enzymes. These data revealed that the most of the enzymes achieved high immobilization yields (> 95 %) when immobilized on AG-Co^{2+} separately. Similar results were found for the co-immobilized systems but for L-AlaDH, whose immobilization yield was lower (77%) when it was co-immobilized with ADH and ωTAs (Table 2).

3

Table 2. Immobilization parameters of single-immobilized and co-immobilized enzymes on AG-Co^{2+}

Heterogeneous Biocatalyst	Enzyme	Immobilized activity (U/g support)[a]	Ψ (%)[b]	Residual specific immobilized activity (%)[c]	Recovered activity (U/g support)[d]
HB-BsADH	BsADH	9.5	95	84	8.0
HB-CvωTA	CvωTA	55	97	20	11
HB-PfωTA	PfωTA	55	96	61	33.4
HB-BsAlaDH	BsAlaDH	96	96	10	9.5
HB3-1-Cv	BsADH	9.6	96	34	3.3
	CvωTA	55	96	22	12
	BsAlaDH	77	77	18	13.8
HB3-1-Pf	BsADH	9.6	96	34	3.3
	PfωTA	57	99	67	38.5
	BsAlaDH	77	77	18	13.8
HB4-1	BsADH	9.6	96	27	2.6
	PfωTA	54	94	52	28.5
	BsAlaDH	97	97	14	13.8
	LpNOX	4.5	99	13	0.57

[a]Immobilized enzymatic activity to 1 g of Ag-Co^{2+} after the immobilization process and according to the difference between the offered solution and the post-immobilization supernatant. [b]Immobilization yield, Ψ = (immobilized activity/offered activity) x 100. [c]Residual specific immobilized activity (%) is defined as the coefficient between the specific activity of the immobilized enzymes and the specific activity of the soluble ones. [d]Residual activity of the enzyme per gram of carrier upon the immobilization process. Specific activity of soluble purified enzymes measured as described in methods: BsADH 0.66 U/mg, PfωTA 7.4 U/mg, BsAlaDH 12.9 U/mg, and LpNOX 1.63 U/mg.

We found a much higher variability among the residual specific activity of the different enzymes upon the immobilization (Table 2). When BsADH was separately immobilized recovers up to 3.5 times more activity than when it was co-immobilized with other enzymes. This effect may be attributed to substrate diffusion restrictions and conformational changes provoked by more crowded environments when co-immobilizing 2 or more enzymes.[28] The molecular crowding within the beads relies on the total protein density upon the immobilization. Hence, HB3-1 presents a 9×10^{-9} nmol x μm^{-3} total density when accounting for the three immobilized enzymes, while HB-BsADH results in a density of 2.5×10^{-9} nmol x μm^{-3} since BsADH was the only immobilized enzyme. Nevertheless, we cannot discard that the other co-immobilized enzymes may provoke some unwanted artifacts (i.e unspecific NADH depletion) in the ADH colorimetric assay. Immobilized CvωTA retained 20-30% of the specific

activity of its soluble counterpart, whereas PfωTA kept 50-60% of activity upon the immobilization.

Finally, the specific activity of BsAlaDH upon the immobilization decreased to less than 20% in all cases (Table 2). The low residual specific activity of all immobilized BsAlaDH biocatalysts may be attributed to the high specific activity of this soluble enzyme,[30] giving rise to heterogeneous biocatalysts with high activity loadings (77-97 U/g) even at low protein loads (1.6 mg $_{protein}$/g$_{carrier}$). These results are aligned with the fact that the immobilization effectiveness dramatically decays with the activity loading.[31]

Next, we assessed the thermal stability of the spatially co-localized heterogeneous biocatalysts by incubating them at 65 ºC under the same cascade reaction conditions (Table 3, Figure. S2). In all cases, the co-immobilized enzymes were more, or similarly, stable than their soluble counterpart. Whereas the co-immobilized PfωTA and BsAlaDH were as stable as the soluble enzymes, the half-life time of the co-immobilized BsADH was 5.4 times higher than the soluble enzyme under high temperature conditions. These stabilizing effects may be attributed to the multi-valent bonding between several His-tags and the carrier surface since all the enzymes forming this system are multimeric. Yet reversible, that multivalency may reinforce the enzyme quaternary structures, preventing their dissociation and consequently their thermal inactivation.[23]

Table 3. Thermal stability of soluble and co-immobilized enzymes at reaction conditions

Enzyme	Half-life time at 65ºC (h)	
	Soluble	Co-immobilized
BsADH	1.29	6.91
CvωTA	0.58	1.04
PfωTA	0.187	0.190
BsAlaDH	1.53	1.83
LpNOX	0.18	0.47

Inactivation conditions were done by incubating biocatalysts in L-Alanine 250 mM, NH$_4$Cl 270 mM, PLP 0.35 mM, DMSO 10% at pH 8.5 at 65ºC. Half-life times were estimated by a 3-parameters biexponential kinetic inactivation model.[29]

4

Co-immoblization of multi-enzyme systems to fabricate multi-functional heterogeneous biocatalysts

Combining the battery of the immobilized enzymes detailed in Table 2, we created two different multi-functional biocatalysts. HB3-3 that contains the three enzymes separately immobilized (HB-ADH, HB- ωTA and HB-LAlaDH) and mixed at the optimal proportions to have the optimal enzyme activity ratio (1:6:10), and HB3-1 where the three enzymes are co-immobilized on the same agarose microbeads keeping the optimal enzyme ratio. In principle, the enzymes forming these two heterogeneous biocatalysts should present different spatial localizations.

The confinement of the three enzymes inside the same porous particle was proven by labelling the enzymes with compatible fluorophores (fluorescenine and rhodamine B) and further performing colocalization studies using confocal laser scanning microscopy (CLSM). Image analytics of these microscopic studies allowed us providing both qualitative and quantitative data about the enzyme localization across the microbead surfaces (Figure 1 and Figure S3-S4).

In the case HB3-1, CLSM studies clearly show that the three co-immobilized enzymes colocalized in all the beads, demonstrating that only one bead population exists (Figure 1B-C and Figure S3A-C). The bead profiles of the confocal planes

unequivocally prove that the three enzymes mainly co-localize at the outer surface of the porous particles (Figure 1E-1F). Quantitative data and colocalization coefficients (Manders and Pearson) support the physical proximity of the enzymes, indicating that >99% of BsAlaDH co-localizes with BsADH and PfωTA, 88 and 99% of BsADH does with BsAlaDH and PfωTA, respectively and >97% of PfωTA co-localizes with both BsAlaDH and BsADH (Figure S4 and Table S2). Besides, image analytics reveal that BsADH, PfωTA and BsAlaDH penetrated into the beads an average of 5.8, 3.5 and 4.5 μm, resulting in densities of 1.7, 5.3 and 14 $\times 10^{-9}$ nmol $\times$ μm^{-3}, respectively, for each enzyme localized in the occupation volume. Similar penetration distances were found for the immobilization of a thermophilic His-tagged ADH on agarose beads activated with nickel-chelates [37a]. According to these densities, we estimated the minimal inter-enzyme distance, assuming a random distribution across the colonized region (see supporting information, Table S3). These data demonstrate that the multi-enzyme system is confined at the outer region of the porous beads with a minimal inter-enzyme distance of 4 nm. On the contrary, CLSM studies of HB3-3 architecture show that the three enzymes are indeed immobilized on separated beads, resulting in three bead populations corresponding to each enzyme (Figure 1A).
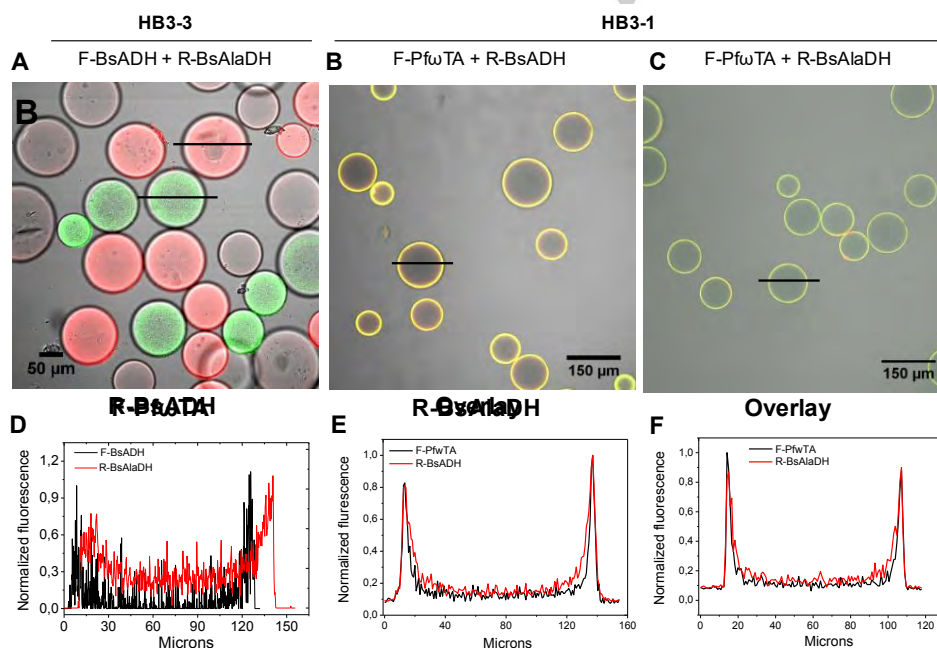

Figure 1. Spatial distribution of the heterogeneous biocatalysts analyzed by CLSM. Overlay fluorescence image of the biocatalyst HB3-3 where BsADH was labelled with fluorescein isothiocyanate (F-BsADH, green), BsAlaDH was labelled with rhodamine B isothiocyanate (R-BsAlaDH, red) and PfωTA remained unlabelled **(A)**. Overlay fluorescence image of the biocatalyst HB3-1 where the transaminase from *Pseudomonas fluorescens* was labelled with fluorescein isothiocyanate (F-PfωTA, green) and the alcohol dehydrogenase from *Bacillus stearothermophilus* was labelled with rhodamine B isocyanate (R-BsADH) **(B)**. Overlay fluorescence images of the biocatalyst HB3-1 where PfωTA was labelled with fluorescein isothiocyanate (F-PfωTA, green) and BsAlaDH was labelled with rhodamine B isothiocyanate (R-BsAlaDH, red) **(C)**. Overlapped normalized intensity profiles from two beads corresponding to HB3-3 sample shown in panel A **(D)** Normalized Intensity profile of one bead corresponding to the HB3-1 sample shown in panel B **(E)** and corresponding to the HB3-1 sample shown in panel C **(F)**. The fluorescence was normalized to the highest intensity value measured in the plot profile.

5

Quantitative studies demonstrated that none enzyme colocalizes with the others within the same bead (Figure S4, Table S2). Noteworthy, single-bead analysis of HB3-3 systems also unveil that BsADH was mainly distributed at the outer surface of the porous beads, although it penetrated up to 9.3 µm, resulting in occupation regions with 1.6 times lower protein density than the same enzyme in the HB3-1 system (Figure 1D, Table S3).

Biosynthesis of benzylamine from benzylalcohol using heterogeneous biocatalysts with different spatial distributions

Encouraged by having two active and stable heterogeneous biocatalysts with different spatial distributions, we exploited them for the biosynthesis of benzylamine from benzyl alcohol. Using low loadings of the heterogeneous biocatalyst at the optimal enzyme ratio, the immobilized system was 2 times slower and reached 3 time less amine yield than the soluble system under the same reaction conditions and enzyme mass (Table 4). This fact is explained by lower specific activity observed for all immobilized enzymes compared to their soluble counterparts (Table 2). To overcome this limitation, we concentrated the crude extract of each enzyme into the carriers, increasing the volumetric protein load without resorting to the time-consuming and energy demanding processes (ultrafiltration, lyophilization…) needed to concentrate soluble crude extracts. Using the same catalysts volume but 5 times higher enzyme mass load, the immobilized multi-enzyme system achieved similar yield and initial rate as the soluble system (Table 1 and 4). Comparing the immobilized systems, HB3-1Cv presented a faster reaction rate and achieved higher benzylamine titer than HB3-3Cv, suggesting that the spatial confinement of three interdependent enzymes enhances the intermediate transfer between the different active sites. When enzymes are immobilized on different particles (HB3-3), NADH and pyruvate have to travel from the beads where they are produced to the beads where LAlaDH is immobilized to enable the cofactor regeneration and avoid the pyruvate accumulation. In contrast, HB3-1 architecture exhibits a higher efficiency likely because cofactor recycling and equilibrium shift occur within the same bead without that journey of intermediates. There are several experimental evidences that demonstrate that confinement of main dehydrogenases and their corresponding recycling partners improve the efficiency of the cofactor recycling.[18, 32] Remarkably, when the ωTA is co-immobilized with an enzyme that recycles the amine donor; L-AlaDH, the equilibrium towards the amination reaction seems to be shifted more efficiently since pyruvate was not accumulated. To the best of our knowledge, the positive effect of spatial co-localization of multi-enzyme system on amination equilibrium shifting was never reported up to now.

We expanded this cascade to the ωTA from *Pseudomonas fluorescens* (PfωTA), since its immobilized version was proven more operationally stable when integrated into packed bed reactors for continuous operations.[25] As shown in table 2, PfωTA was quantitatively immobilized on AG-Co^{2+}, expressing roughly 60% of its specific activity in both co-immobilized (HB3-1Pf) and separately immobilized (HB3-1Pf) biocatalysts. These results match with the immobilization parameters reported for the same enzyme immobilized on polymethacrylate resins activated with epoxy-Co^{2+} groups.[25] All multi-functional heterogeneous biocatalysts incorporating PfωTA enhanced the reaction rate and reached higher amine yields than those containing CvωTA (Figure. S5).

Table 4. Effect of enzyme load in the performance of heterogeneous multi-enzymatic systems synthesizing benzylamine starting from benzyl alcohol

Heterogeneous Biocatalysts	Carrier loading (mg) / (%)	Rate (µM/min)	SSP[c] (µM/min x mg$_{BsADH}$)	Benzylamine yield (%)
HB3-3Cv	60 (3.8)[a]	5.0	17	9
	300 (16)[b]	16	11	30
HB3-1Cv	20 (1.3)[a]	5.5	27	10
	100 (6.3)[b]	27	18	49

All reactions were carried out in 1.5 mL Bio-spinTM chromatographic column where immobilized enzymes were placed and mixed at a final volume of 1.5 mL with a reaction mixture consisted of 50 mM of benzyl alcohol at pH 8.5 with NAD$^+$ 0.75 mM, PLP 0.35 mM, L-Alanine 250 mM, NH$_4$Cl 275 mM and DMSO 10%; incubated at 40 rpm at 25ºC. Conversions were measured after 15 h of reaction. The relative catalyst loading in percentage was calculated by dividing the mass of the heterogeneous biocatalyst added to the reaction, between the reaction volume plus the volume occupied by the mass of the biocatalyst. [a] The heterogeneous biocatalyst contains 0.2 U of BsADH (0.30 mg), 1.16 U CvωTA and 2 U BsAlaDH. [b] The heterogeneous biocatalyst contains 1 U of BsADH (1.5 mg), 5.8U CvωTA and 10 U BsAlaDH. In both cases the enzyme ratio was 1:6:10 (BsADH:CvωTA:BsAlaDH). [c] SSP: Specific system productivity defined as the initial rate divided by the mass amount of BsADH in the reaction.

6

The better performance observed for the tetrameric transaminase from *Pseudomonas* is supported by both biochemical and operational studies that demonstrate its higher stability compared to the transaminase from *Chromobacterium*.[25-26, 33] Those stability differences mainly rely on the higher affinity of PfωTA towards PLP that stabilizes its active holoform.

An insightful study under different cofactor concentrations demonstrates that the enzyme colocalization affects the cascade performance in a different manner, depending on the used transaminase (Figure. 2A and S5). Using 66-fold less cofactor (NAD+ 0.75 mM) than alcohol, HB3-1Pf and HB3-3Pf presented slightly higher initial rates and benzylamine yields, while HB3-1Cv produced 2.1-fold more aminated compound and was 1.5 times faster than HB3-3Cv. When BsADH and LAlaDH were co-

immobilized but segregated from the immobilized PfωTA, both rate and product yield were similar to those observed when the three enzymes were immobilized on three separated beads (Table S4).

On the contrary, using a 500 excess of benzyl alcohol over the cofactor (NAD+ 0.1 mM), we observed that co-immobilized multi-enzyme system remarkably enhanced the cascade performance, (Figure 2B). For both CvωTA and PfωTA, the co-immobilized system (HB3-1) enhanced 1.8-fold the amine yield and performed the reaction 1.5-times faster than the system spatially segregated (HB3-3). However, that low cofactor concentration provoked a significant decreasing of the benzylamine yield as observed in other system driven by NAD(P)H dependent alcohol dehydrogenases,[34] reductases and oxygenases.[35]
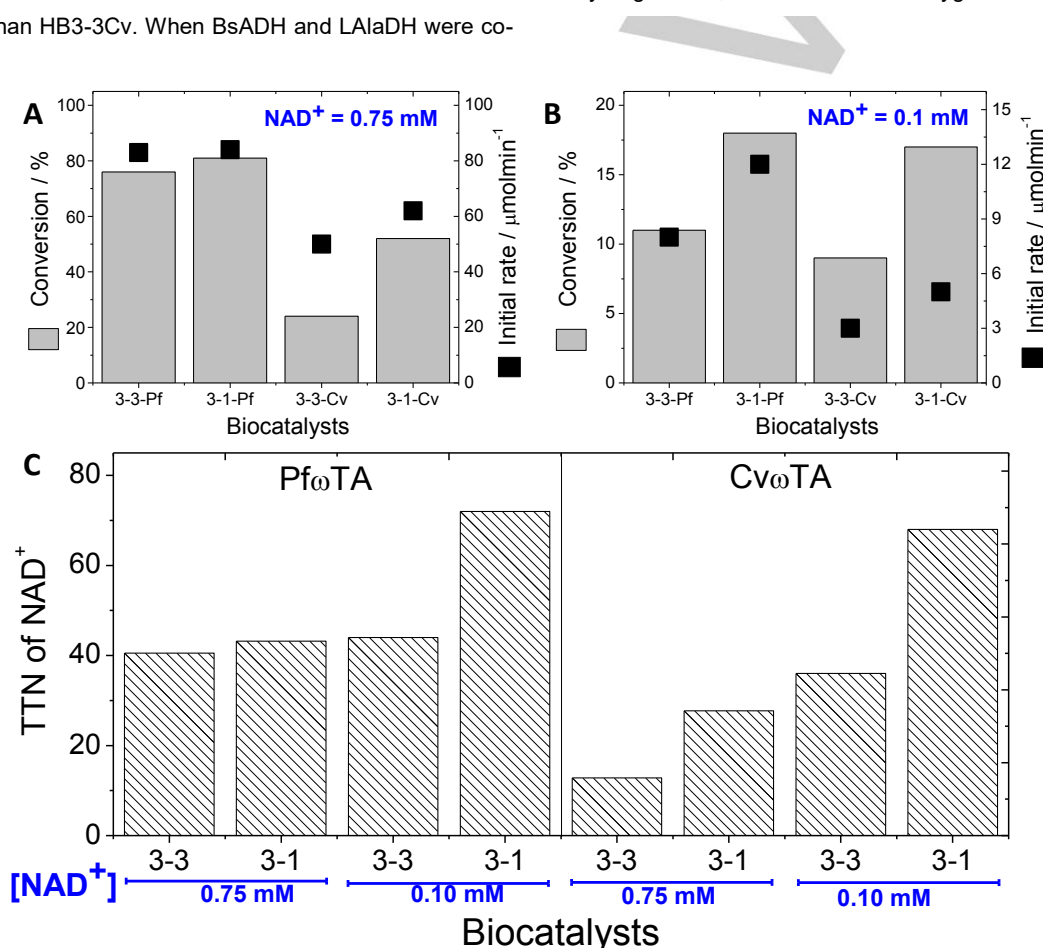

Figure 2. Effect of enzyme distribution on the performance of multi-functional heterogeneous biocatalyts. Final conversion and the initial rates at non limited (**A**) and limited (**B**) cofactor concentrations. **C**) Total turnover number of NAD+ at not limiting and limiting cofactor concentrations. All reactions were carried out with a reaction mixture consisted of 50 mM of benzyl alcohol at pH 8.5 with NAD+, PLP 0.35 mM, L-Alanine 250 mM, NH4Cl 275 mM and DMSO 10%; incubated at 40 rpm at 25 ºC. Conversions were measured after 17 h of reaction. All reactions were carried out using heterogeneous biocatalysts with the same enzyme mass loads.

When the cofactor recycling efficiency was assessed by calculating the total turnover number (TTN) of NAD+, we confirmed that product yields and rates were linked to the NAD+

recycling efficiency (Figure. 2C). Using PfωTA, we found similar TTN (≈ 40) for both HB3-1Pf and HB3-3Pf architectures under higher but still sub-stoichiometric amounts of NAD+, unlike using

7

CvωTA, where the cofactor TTN calculated for HB3-1Cv was 2.2 times higher than for HB3-3Cv. Under much limiting NAD$^+$ conditions, we observed a similar trend for both CvωTA and PfωTA; the co-immobilized systems recycle the cofactor more efficiently. Hence, HB3-1Pf doubles the TTN value of HB3-3Pf, reaching a maximum number of 70. Therefore, the colocalization of BsADH, PfωTA and BsAlaDH on AG-Co^{2+} resulted in a multi-functional heterogeneous biocatalyst able to perform the oxidation/transamination cascade at both highest rate and product yield.

These results suggest that the cascades including PfωTA are mainly limited by the cofactor recycling rather than by the equilibrium shift. Hence, the cascade yield and rate only suffer significant efficiency losses when the enzymes are separated and the reaction is performed at low cofactor concentrations. However, cascades integrating CvωTA seem to be limited by both cofactor recycling and equilibrium shift, since spatial enzyme segregation drive to lower cascade efficiencies under both limiting and non-limiting cofactor conditions. Moreover, the effective co-localization of the three enzymes enhances the cofactor recycling as reflected by the higher TTN numbers, overall for those conditions where NAD$^+$ concentration is rather low. Therefore, the intraparticle shuttling of benzaldehyde and recycling of both redox cofactor and amine donor speed up the transformation of benzyl alcohol (ΔG°= -8.3±0.8 kcal/mol) into benzylamine (ΔG°= +35.3±0.8 kcal/mol), even reaching high yields despite being a thermodynamically challenging cascade.[36] These results align with other NAD(P)H dependent cascades where the cofactor recycling efficiency has been enhanced through the co-immobilization of ADH and reductases on a variety of carriers functionalized with different reactive groups.[37]
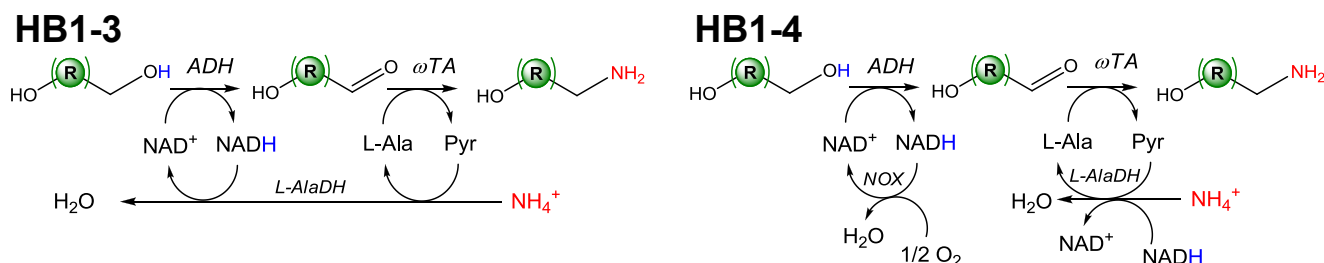
Synthesis of different aminoalcohols from diols

We evaluated the versatility of both HB3-1Pf and HB3-1Cv to synthesize a battery of aliphatic and aromatic aminoalcohols starting from different diols. According to the results obtained for the synthesis of benzylamine, HB3-1Pf catalyzes the cascade reaction more efficiently than HB3-1Cv, achieving higher aminoalcohol yields in all cases (Table 5). The highest aminoalcohol yields were achieved starting from short, linear and aliphatic diols. 66 % of **1s** was transformed into **1p** in 41 h

detecting less than 2% of the intermediate (hydroxyaldehyde). Unlike the whole-cell and soluble cell-free cascades involving ADH, AlaDH and ωTA, the immobilized system did not produce the corresponding diamines. The low accumulation of the intermediates and unwanted overaminated products supports that the cofactor regeneration is limited by the transamination step, since the ωTA provides the pyruvate required by the BsAlaDH to recycle both the NAD$^+$ and L-Ala pools demanded by the ADH and ωTA, respectively.

Larger diols with higher substitution grade were worse starting materials for the immobilized multi-enzyme system as reported elsewhere for the soluble enzyme cascade.[12] Noteworthy, *p*-substituted aromatic diols and 1,2 vicinal diols were poorly transformed mainly due to the poor activity of native BsADH and ωTAs towards these substrates and intermediates, respectively (Table S5). In the future, we plan exploiting engineered ωTAs with improved activity towards bulky substrates,[38] to expand the synthetic capabilities of this immobilized system.

Decoupling the cofactor regeneration from the transamination step might enhance the cascade performance increasing the aminoalcohol yields. To that aim, we co-immobilized a fourth enzyme; a water-forming NADH oxidase from *Lactobacillus pentosus* (LpNOX)[39] that recycles NAD$^+$ without interplaying with the ωTA/BsAlaDH pair. The biocatalyst resulting of co-immobilizing His-tagged BsADH, LpNOX, PfωTA and BsLAlaDH on AG-Co^{2+} was named as HB4-1 and showed the same colocalization pattern as HB3-1 architectures (Figure S3-4). Noteworthy, immobilized LpNOX was almost 2-times more stable than its soluble counterpart (Table 3). Adding LpNOX to the cascade enhanced the BsADH activity since the cofactor recycling became independent of both transamination and reductive amination steps. HB4-1 architecture took 17 hours to yield similar or even higher aminoalcohol yields than those obtained with HB3-1 after 41 hours. These higher yields are the consequence of higher conversions of the starting diol (up to 95% for **1s** after 41 hours) which resulted in significant accumulation of the hydroxyaldehyde intermediates (Table S6). The integration of LpNOX demonstrates that ωTA is the limiting enzyme of this oxidation/amination cascade, since diols are more efficiently oxidized in presence of LpNOX.

8

Table 5. Synthesis of aminoalcohols from diols catalyzed by heterogeneous co-immobilized biocatalysts on AG-Co^{2+} microbeads.

Diol	Amino alcohol	HB3-1-Cv			HB3-1-Pf			HB4-1		
			Yield [b] (%)			Yield [b] (%)			Yield [b] (%)	
			Time (h)			Time (h)			Time (h)	
		Rate[a]	17	41	Rate[a]	17	41	Rate[a]	17	41
1s	1p	3.53	24	24	5.74	39	66	8.68	59	59
2s	2p	0.88	6	6	1.32	9	14	4.26	29	31
3s	3p	1.32	9	11	1.47	10	11	2.50	17	17
(S)-3s	(S)-3sp	na	na	na	Na	na	na	0	na	17
4s	4p	na	na	na	Na	na	na	1.18	8	21
5s	5p	0	0	0	0	0	0	0	0	0
6s	6p	0.30	na	5	0.55	na	9	0.37	na	6

All reactions were carried out in 1.5 mL Bio-spinTM chromatographic column where 75 mg of biocatalyst were placed with 375 µL of reaction mixture consisted of 50 mM of substrate at pH 8.5 with NAD+ 0.75 mM, PLP 0.35 mM, L-Alanine 250 mM, NH$_4$Cl 275 mM, DMSO 10% and incubated at 40 rpm at 25 ºC. FAD+ 150 µM was also added to the reaction mixture for HB4-1. na: not assessed. The biocatalyst HB4-1 bears PfωTA. [a]Rate: µmol$_{aminoalcohol}$ x h^{-1} x g$_{biocatalyst}$$^{-1}$. The rate was calculated using the conversion after 17 hours of reaction. [b] Aminoalcohol yield at different times.

For the synthesis of **2-4p**, decoupling the oxidation from the transamination allowed increasing the product yields in shorter times.

Although the enantioselectivity was out of the scope of this work, we studied the performance of the cascade starting with chiral diols like (S)-**3s**. As result, we obtained a similar aminoalcohol yield when using that enantiopure diol as using the racemic mixture. Hence, immobilized cascade expectedly shows an enantiopreference for the *S*-enantiomer according to the PfωTA selectivity.

Remarkably, the yield of **1p** was slightly lower in presence of LpNOX, yet the reaction rate was almost doubled when the NADH oxidase was integrated into the system. This particular effect may be explained by the unpaired activity of BsADH boosted by LpNOX that consumes much faster the diol accumulating higher concentrations of 3-hydroxy propanal and consequently decreasing the amino donor:acceptor ratio, which hampers the transamination equilibrium as previously reported.[19] Moreover, LpNOX also competes with BsAlaDH for the NADH inhibiting its capacity to shift the equilibrium towards the amination reaction through the regeneration of the amino donor.

Previous to this work, the only example of immobilized multi-enzyme system to manufacture aminoalcohols was based on transketolases and transaminases.[40] This system exclusively performed the synthesis of 2-amino-1,3,4-butanediol with a 10% conversion regarding to the starting materials and using a two packed bed bioreactors connected in line. Pleasantly, the system we present here spatially confines all the enzymes participating in the cascade, yields up to 66% of short linear 1,ω-aminoalcohols in one-pot and also works with a diversity of diols.

Operational stability of multi-functional heterogeneous biocatalyst

We evaluated the recyclability of HB4-1 biocatalyst by reusing it in consecutive batch cycles. In this scenario, after 3 consecutive 24 h cycles, the biocatalyst maintains 90 and 60% of its initial performance for the synthesis of benzylamine and **1p**, respectively. After six cycles, the biocatalyst HB4-1 decreased its initial performance by 70% (Figure. 3). The lower yields after the last cycle were mainly attributed to the PfωTA and LpNOX inactivation as demonstrated by *ex-situ* activity colorimetric assays (Table S7). The activity losses found for these enzymes

9

were likely due to structural distortions during the operational process. These conformational changes are supported by the protein intrinsic fluorescence spectrum recorded after the operational utilization of HB4-1 (Figure S6). The heterogeneous biocatalyst presented a lower maximum overall fluorescence intensity, which suggests some structural distortions of the immobilized proteins that may explain the system inactivation after its operational utilization. When CvωTA was used as transaminase instead PfωTA, the operational stability of the multi-functional heterogeneous biocatalysts was far lower (Figure S7).
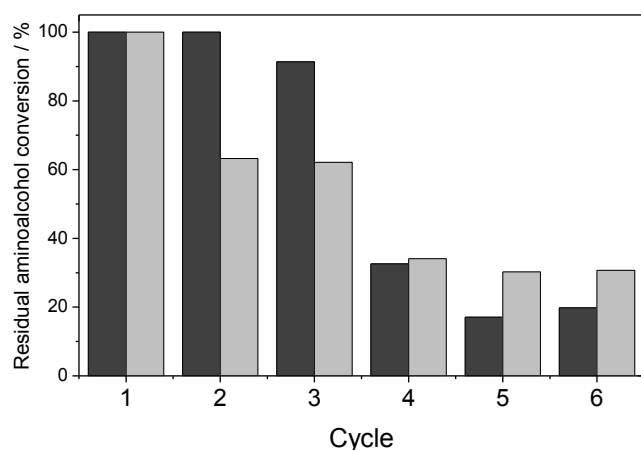

Figure 3. Operational stability of multi-functional heterogeneous biocatalyst (HB4-1) by repeated batch cycles. All reactions were carried out in 1.5 mL Bio-spin™ chromatographic column where 75 mg of biocatalyst HB4-1 were placed with 375 μL of reaction mixture consisted of 50 mM of substrate at pH 8.5 with NAD⁺ 0.75 mM, PLP 1 mM, L-Alanine 250 mM, NH₄Cl 275 mM and DMSO 10%; incubated at 40 rpm at 25ºC. Benzyl alcohol (dark gray bars) and 1,3-propanediol (light gray bars).

Conclusion

We have prepared a cell-free multifunctional heterogeneous biocatalyst to manufacture aminoalcohols from diols in one-pot. The co-immobilized system integrates a redox-self-sufficient cascade where cofactor and amino donor are efficiently recycled, producing water as by-product. This heterogeneous biocatalyst presented a broad substrate scope but showed preference towards non vicinal short aliphatic diols. Besides, the immobilized biocatalyst can be used in repeated batch cycles. Breaking the redox neutrality, we were able to increase the maximum yields and the production rates for the vast majority of the tested aminoalcohols. Our future efforts aim at broadening the substrate scope and to enhance the stability of the ωTAs and NOX enzymes, whose extremely low stabilities meant the major bottleneck for this cascade. In this study, we demonstrate the importance of precisely co-localized immobilized enzymes

and tuning their enzyme ratios when performing step-wise biotransformations in one-pot. Additionally, this study reveals the intimate relation between the spatial distribution of immobilized enzyme cascade and the efficiency of cofactor recycling and equilibrium shifts; two processes often demanded in biosynthetic pathways. This work contributes to increase the toolbox of heterogeneous biocatalysis to synthesize valuable building blocks and helps to understand how spatial distribution of immobilized enzyme systems affects their efficiency.

Experimental Section

Chemicals

Substrates as benzyl alcohol, benzaldehyde, benzyalmine, 1,3-propanediol (**1s**), 1-4-butanediol (**2s**), 1,3-butanediol (**3s**), *S*-1,3-butanediol [**(S)-3s**], 3-methyl-1,5-pentanediol (**4s**), glycerol (**5s**) and 4-hydroxybencyl alcohol (**6s**); standards as 3-amino-1-propanol (**1p**), 4-amino-1-butanol (**2p**), 4-amino-2-butanol (**3p**), 3-methyl-5-amino-1-pentanol (**4p**), 3-amino-1,2-propanediol (**5p**) and 4-hydroxybenzylamine (**6p**); other reagents as dihydroxyacetone (DHA), aldol, glyceraldehyde, kanamycin sulfate from *Streptomyces kanamyceticus*, ampicillin, flavin-adenine-dinucleotide sodium salt (FAD⁺), pyridoxal 5′-phosphate monohydrate >97% (PLP), fluorescein isothiocyanate (FITC), rhodamine B isothiocyanate, acetic anhydride and n-methylimidazole were acquired from Sigma-Aldrichs (St. Lous, IL, USA). Isopropyl β-D-thiogalactopyranoside (IPTG), Nicotinamide adenine dinucleotide reduced disodium salt (NADH), nicotinamide adenine dinucleotide sodium salt (NAD⁺), were purchased from GERBU Biotechnik GmbH (Wieblingen, Germany). Cobalt-activated agarose microbeads 4BCL (AG-Co²⁺) (particle size; 50-150 μm, pore size; 112 nm (mean value) and 15μmol of Co^{2+} x $g_{carrier}^{-1}$) were purchased from ABT technologies (Madrid, Spain). Precision plus protein™ standards, micro Bio-spin™ chromatographic columns and Bradford reagent were acquired from BIORAD. All other reagents and solvents were analytical grade or superior.

Cloning of his-tagged water forming NADH oxidase variants from Lactobacillus pentosus *(Lp-NOX)*

The gene described by Nowak *et al.*[41] was optimized for *E. coli* codon usages and synthesized by Genscript Biotech (Piscataway, NJ, USA). The synthetic gen was cloned into pET28b(+) using NdeI and XhoI restriction sites. DNA isolation, plasmid purification, restriction analysis, plasmid construction and DNA sequencing were carried out by standard methods.[42]

Bacterial strains and growth conditions

Alcohol dehydrogenase from *Bacillus Stearothermophilus*, ω-transaminases from *Pseudomonas fluorescens* and *Chromobacterium violaceum*, L-alanine dehydrogenase from *Bacillus subtilis*, were cloned and overexpressed in competent *E. coli* BL21 cells transformed with the respective plasmid as previously reported.[23, 25-26] Briefly, 1 mL of an

10

overnight culture of *E. coli* BL21(DE3) harboring each plasmid was used to inoculate 50 mL of Luria-Bertain (LB) medium containing the corresponding antibiotic; kanamycin (final concentration 30 µgmL^{-1}) was used for all enzymes but CvωTA that required ampicillin (final concentration 50 µgmL^{-1}). The resulting culture was aerobically incubated at 37 ºC with orbital shaking at 250 rpm until the OD600nm reached 0.6. Afterwards, the culture was induced with 1 mM IPTG. All enzymes were induced for 3h at 37ºC but CvωTA that was incubated at 21 ºC for 18 h. After the induction time, cells were harvested by centrifugation at 4211 g for 30 min at 4 ºC. Supernatants were discarded and the pellet was resuspended in 5 mL of 25 mM sodium phosphate buffer solution at pH 7, unless cells expressing ωTAs that were resuspended in 25 mM HEPES buffer at pH 8 containing 1 mM PLP. Cells were broken by sonication using a Sonoplus Serie 4200, Bandelin at 20% amplitude (5 s ON / 5 s OFF) for 20 min at 4 ºC. The suspension was then centrifuged at 10,528 g for 30 min at 4 ºC and the pellet was discarded. The supernatant containing cell extracts with the His-tagged proteins were collected and employed for further purification and/or immobilization.

Purification and immobilization of enzymes

10 volumes of crude cell extract containing the His-tagged enzymes were mixed with 1 volume of AG-Co^{2+} microbeads and incubated under orbital shaking for 1 to 2 h at 4 ºC. Later, the suspension was filtered and the microbeads containing the enzyme were washed with 5 volumes of 25 mM phosphate buffer at pH 7 for all enzymes but ωTAs that were washed with 25 mM HEPES buffer at pH 8 containing 1 mM PLP. These resins were stored at 4º C for performing the biotransformation (Figure. S1).

Enzymatic activity measurements

Enzyme activities were spectrophotometrically measured in transparent 96-well microplates, employing a Microplate Reader Epoch 2, BioTek® with the software Gen5.

ADH activity

200 µL of a reaction mixture containing 100 mM benzyl alcohol, 1 mM NAD$^+$, DMSO 10 % in sodium bicarbonate buffer at pH 9 were incubated with 5 µL of enzymatic solution or suspension at 30 ºC. The increase in the absorbance was monitored at 340 nm. One unit of activity was defined as the amount of enzyme that was required to either reduce 1 µmol of NAD$^+$ per minute at the assayed conditions.

L-AlaDH activity

200 µL of a reaction mixture containing 75 mM sodium pyruvate, 500 mM NH$_4$Cl, 0.5 mM NADH, in 100 mM phosphate buffer at pH 8 and DMSO 10% at 30 ºC were incubated with 5 µL of enzymatic solution or suspension at 25 ºC. The decrease in the absorbance at 340 nm was monitored. One unit of activity was defined as the amount of enzyme that was needed to produce 1 µmol of L-alaine per minute at the assayed conditions.

ωTA activity

The activity was determined by recording the decrease in the absorbance at 245 nm of 200 µL of a reaction mixture containing benzaldehyde (1.2 mM), L-alanine (500 mM), PLP (0.1 mM), DMSO 10% in bicarbonate buffer 100 mM pH 8.5. The reaction was initiated by adding 5 µL of the enzymatic solution or suspension to the reaction mixture. One unit of ωTA activity was defined as the amount of enzyme required for the production of one µmol of benzylamine per minute at the assessed conditions.

NOX activity

200 µL of a reaction mixture containing 0.2 mM NADH, 150 µM FAD$^+$, DMSO 10% in phosphate buffer pH 8 at 30 ºC were incubated with 5 µL of enzymatic solution or suspension at 30 ºC. The decrease in the absorbance was monitored at 340 nm. One unit of activity was defined as the amount of enzyme that was required to oxidize 1 µmol of NADH per minute at the assayed conditions.

Enzyme immobilization

Separately immobilized enzymes were prepared by mixing 10 volumes of crude cell extract containing the His-tagged protein with 1 volume of AG-Co^{2+} microbeads and incubated under orbital shaking for 1-2 h at 4 ºC. Later, the suspension was filtered and the microbeads containing the enzyme were washed with 5 volumes of 25 mM phosphate buffer at pH 7 or 25 mM HEPES buffer at pH 8 containing 1 mM PLP when working with ωTAs. The immobilized biocatalyst was stored at 4 ºC. On the other hand, co-immobilized enzymes were prepared by consecutively immobilizing each enzyme one-by-one in the following order: *HB3-1Cv:* 1st BsADH, 2nd BsAlaDH, 3rd CvωTA; *HB3-1Pf:* 1st BsADH, 2nd BsAlaDH, 3rd PfωTA; *HB4-1:* 1st BsADH, 2nd BsAlaDH, 3rd LpNOX, 4th PfωTA. To immobilize each enzyme, we follow the same methodology as described previously with the separately immobilized enzymes.

For both immobilization protocols the purity of the enzymes was checked. Firstly, the proteins were eluted by the addition of 5 volumes of 300 mM imidazole in the respective buffer and incubating for 1 h at 4 ºC with orbital shaking. The eluted protein was dialysate to remove the imidazole. Finally, SDS-PAGE and Bradford protein assay[43] were carried out after each production to determine the purity, concentration and specific activity of the enzymes.

Protein labeling with fluorescent probes

Fluorescent labeling was done accordingly with a methodology reported elsewhere.[44] An enzyme solution in 100 mM of sodium bicarbonate buffer at pH 9.5 was mixed (1:20 molar ratio) with FITC or rhodamine B isothiocyanate solution in DMSO (10 mg/mL) and incubated 1 h with gentle agitation at 25 ºC in darkness. Later, the remaining FITC or rhodamine was eliminated by filtering the enzyme solution in a tangential ultrafiltration unit (10 kDa) with a 25 mM sodium phosphate buffered solution at pH 7 until no coloration was observed in the filtered solution.

Confocal laser scanning microscopy (CLSM) imaging

The localization and distribution of fluorophore-labelled enzymes immobilized along the AG-Co^{2+} microbeads were analyzed with a confocal microscope Espectral ZEISS LSM 880 with an excitation laser (λ_{ex}: 488 nm for FITC and λ_{ex}: 561 nm for Rhodamine B) and emission

11

filter (LP505 and LP565, respectively). Image processing was done with the program FIJI.

Enzyme co-localization analysis

ICA plots of different co-localized enzymes within the porous surface of AG-Co^{2+} microbeads were obtained analyzing the CLSM images with FIJI, using the plugin JaCoP. Pearson Manders and correlation intensity coefficient were determined through analyzing the CLSM images with FIJI using the plugin JaCoP.[45]

Thermal inactivation

Inactivation of both soluble and immobilized enzymes were carried out by incubating a suspension or solution of enzymes at pH 8.5 with NAD$^+$ 0.75 mM, PLP 0.35 mM, L-alanine 250 mM, NH$_4$Cl 275 mM and DMSO 10% at 65ºC. In order to calculate half-life times, the obtained experimental measurements were adjusted to a 3-parameters biexponential kinetic inactivation model.[29]

Synthesis of aminoalcohols

75 mg of immobilized biocatalysts were placed inside a 1.5 mL Bio-spin^{TM} chromatographic column with 375 µL of reaction mixture consisted of 50 mM of substrate (1s, 2s, 3s, S-3s, 4s, 5s or 6s) at pH 8.5 with NAD$^+$ 0.75 mM, PLP 0.35 mM, L-Alanine 250 mM, NH$_4$Cl 275 mM, DMSO 10% and incubated at 25 ºC in a vertical rotating shaker at 40 rpm. When LpNOX was present, reaction mixture was supplemented with FAD$^+$ 150 µM. Reaction curse was monitoring by withdrawing samples at periodic intervals which were analyzed by chromatographic methods.

Chromatographic methods
High Performance Liquid Chromatography (HPLC)

Before their analysis, samples were filtered and diluted in the mobile phase (ammonia 0.1% in water/acetonitrile, 80:20). Prepared samples were analyzed by HPLC (Waters 2690) with a Luna® 5 µm C18 (2) 100 Å (150 x 4.6 mm) Phenomenex column, equipped with a PDA detector at 245 nm. Analytes were eluted at 0.75 mL x min^{-1} constant flow with a reverse mobile phase composed by solvent A: acetonitrile and B: 0.1 % ammonia in water, with the following gradient (A:B): 30:70 from 0-12 min, 36:64 from 12-13 min and 30:30 from 14-16 min. Retention times were benzyl alcohol: 5.5 min, benzylamine: 6.3 min and benzaldehyde: 11.0 min.

Gas chromatography (GC)

Prior GC analysis, samples were derivatized as described elsewhere.[46] Briefly, 30 µL of aqueous reaction simple were placed in a 1.5 mL Eppendorf tube, followed by the addition of 30 µL of n-methylimidazole and 225 µL of acetic anhydride and incubated by 10 min at room temperature. Afterwards, 300 µL of distilled water was added to cool down to cool down and stop the derivatization reaction. Later, liquid-liquid extraction of acetylated compounds was done by the addition of 300 µL of dichloromethane discarding the aqueous phase. 30-50 mg of anhydrous MgSO$_4$ were added to dry samples before GC analysis. As internal standard, eicosane 2 mM was employed. Gas chromatography analyses were carried out in a Hewlett Packard 7890 series II gas chromatograph using a column of phenyl silicone 5.5% (Zebron ZB-5HT

Inferno 30 m × 0.25 mm × 0.25 µm), helium as a carrier gas, and equipped with a flame ionization detector (FID). Injector at 210 ºC, FID detector at 250 ºC. Separation of compounds were by the following temperature ramp: initial temperature at 140 ºC, maintained 2 min, ramp to 240 ºC at a rate of 20 ºC/min and finally maintained 2 min. Retention times for acetylated compounds are **1s**: 2.82 min, **1p**: 4.22 min, **2s**: 3.34 min, **2p**: 5.13 min, **3s**: 2.90 min, **3p**: 4.27 min, (**S**)-**3s**: 2.90 min, (**S**)-**3p**: 4.27 min, **4s**: 4.30 min, **4p**: 6.20 min, **5s**: 4.24 min, **5p**: 5.80 min, **6s**: 5.67 min, **6p**: 7.45 min, DHA: 3.36 min, aldol: 2.84 min and eicosane: 8.21 min.

Operational stability of biocatalyst

75 mg of HB4-1 were placed inside a 1.5 mL Bio-spin^{TM} chromatographic column with 375 µL of reaction mixture consisted of 50 mM of substrate (benzyl alcohol or **1s**) at pH 8.5 with NAD$^+$ 0.75 mM, PLP 1 mM, FAD$^+$ 150 µM, L-Alanine 250 mM, NH$_4$Cl 275 mM and DMSO 10%; incubated at 25 ºC in a vertical rotating shaker at 40 rpm. After each reaction cycle (24 h), columns were spin down and washed one time with one volume of 25 mM HEPES buffer at pH 8.5 with 0.1 mM PLP before start the next reaction cycle. Recovered reaction mixtures were analyzed as described in the chromatographic methods.

[1] H. A. Wittcoff, B. G. Rueben, J. S. Plotkin, *Industrial Organic Chemicals* Wiley- Interscience, New York, **2004**.
[2] R. N. Patel, *Biomolecules* **2013**, *3*, 741-777.
[3] a) D. Ghislieri, N. J. Turner, *Top. Catal.* **2014**, *57*, 284-300; b) S.-L. Shi, Z. L. Wong, S. L. Buchwald, *Nature* **2016**, *532*, 353; c) A. Fischer, T. Mallat, A. Baiker, *J. Mol. Catal. A: Chem.* **1999**, *149*, 197-204.
[4] R. C. Rodrigues, C. Ortiz, A. Berenguer-Murcia, R. Torres, R. Fernández-Lafuente, *Chem. Soc. Rev.* **2013**, *42*, 6290-6307.
[5] a) F. Lopez-Gallego, C. Schmidt-Dannert, *Curr. Opin. Chem. Biol.* **2010**, *14*, 174-183; b) J. H. Schrittwieser, S. Velikogne, M. Hall, W. Kroutil, *Chem. Rev.* **2018**, *118*, 270-348; c) R. C. Simon, N. Richter, E. Busto, W. Kroutil, *ACS Catal.* **2014**, *4*, 129-143; d) F. López-Gallego, E. Jackson, L. Betancor, *Chem. Eur. J.* **2017**, *23*, 17841-17849; e) M. P. Thompson, I. Peñafiel,

12

S. C. Cosgrove, N. J. Turner, *Org. Procces Res. Dev.* **2019**, *23*, 9-18.

[6] S. Klatte, V. F. Wendisch, *Biorg. Med. Chem.* **2014**, *22*, 5578-5585.

[7] K. Hernandez, J. Bujons, J. Joglar, S. J. Charnock, P. Domínguez de María, W. D. Fessner, P. Clapés, *ACS Catal.* **2017**, *7*, 1707-1711.

[8] J.-D. Zhang, X.-X. Yang, Q. Jia, J.-W. Zhao, L.-L. Gao, W.-C. Gao, H.-H. Chang, W.-L. Wei, J.-H. Xu, *Catal. Sci. Technol.* **2019**, *9*, 70-74.

[9] a) M. F. Villegas-Torres, R. J. Martinez-Torres, A. Cázares-Körner, H. Hailes, F. Baganz, J. Ward, *Enzyme Microb. Technol.* **2015**, *81*, 23-30; b) P. Gruber, F. Carvalho, M. P. C. Marques, B. O'Sullivan, F. Subrizi, D. Dobrijevic, J. Ward, H. C. Hailes, P. Fernandes, R. Wohlgemuth, F. Baganz, N. Szita, *Biotechnol. Bioeng.* **2018**, *115*, 586-596; c) C. U. Ingram, M. Bommer, M. E. B. Smith, P. A. Dalby, J. M. Ward, H. C. Hailes, G. J. Lye, *Biotechnol. Bioeng.* **2007**, *96*, 559-569.

[10] A. Pellis, S. Cantone, C. Ebert, L. Gardossi, *N. Biotechnol.* **2018**, *40*, 154-169.

[11] S. Wu, Z. Li, *ChemCatChem* **2018**, *10*, 2164-2178.

[12] J. H. Sattler, M. Fuchs, K. Tauber, F. G. Mutti, K. Faber, J. Pfeffer, T. Haas, W. Kroutil, *Angew. Chem. Int. Ed.* **2012**, *51*, 9156-9159.

[13] O. Barbosa, C. Ortiz, Á. Berenguer-Murcia, R. Torres, R. C. Rodrigues, R. Fernandez-Lafuente, *Biotechnol. Adv.* **2015**, *33*, 435-456.

[14] C. Schmidt-Dannert, F. Lopez-Gallego, *Microb. Biotechnol.* **2016**, *9*, 601-609.

[15] a) S. Velasco-Lozano, F. López-Gallego, *Biocatal. Biotransform.* **2017**, 1-11; b) C. Schmid-Dannert, F. López-Gallego, *Curr. Opin. Chem. Biol.* **2019**, *49*, 97-104; c) J. Britton, S. Majumdar, G. A. Weiss, *Chem. Soc. Rev.* **2018**, *47*, 5891-5918; d) L. Tamborini, P. Fernandes, F. Paradisi, F. Molinari, *Trends Biotechnol.* **2018**, *36*, 73-88.

[16] R. Sigrist, B. Z. D. Costa, A. J. Marsaioli, L. G. de Oliveira, *Biotechnol. Adv.* **2015**, *33*, 394-411.

[17] F. López-Gallego, in *Methods Enzymol, Vol. 617* (Eds.: C. Schmidt-Dannert, M. B. Quin), Academic Press, **2019**, pp. 385-411.

[18] S. Ren, C. Li, X. Jiao, S. Jia, Y. Jiang, M. Bilal, J. Cui, *Chem. Eng. J.* **2019**, *373*, 1254-1278.

[19] R. Abu, J. M. Woodley, *ChemCatChem* **2015**, *7*, 3094-3105.

[20] F. Guo, P. Berglund, *Green Chem.* **2017**, *19*, 333-360.

[21] a) K. Tauber, M. Fuchs, J. H. Sattler, J. Pitzer, D. Pressnitz, D. Koszelewski, K. Faber, J. Pfeffer, T. Haas, W. Kroutil, *Chem. Eur. J.* **2013**, *19*, 4030-4035; b) M. D. Truppo, J. D. Rozzell, J. C. Moore, N. J. Turner, *Org. Biomol. Chem.* **2009**, *7*, 395-398.

[22] F. López-Gallego, L. Yate, *Chem. Commun.* **2015**, *51*, 8753-8756.

[23] E. S. da Silva, V. Gómez-Vallejo, J. Llop, F. López-Gallego, *Process Biochem.* **2017**.

[24] U. Kaulmann, K. Smithies, M. E. B. Smith, H. C. Hailes, J. M. Ward, *Enzyme Microb. Technol.* **2007**, *41*, 628-637.

[25] A. I. Benítez-Mateos, M. L. Contente, S. Velasco-Lozano, F. Paradisi, F. López-Gallego, *ACS Sustain. Chem. Eng.* **2018**, *6*, 13151-13159.

[26] D. Roura Padrosa, R. Alaux, P. Smith, I. Dreveny, F. López-Gallego, F. Paradisi, *Front. Bioeng. Biotech.* **2019**, *7*.

[27] A. I. Benítez-Mateos, E. Mehravar, S. Velasco-Lozano, L. Salassa, F. López-Gallego, RadmilaTomovska, *Molecules (Basel, Switzerland)* **2019**, *24*.

[28] a) M. Feig, I. Yu, P.-h. Wang, G. Nawrocki, Y. Sugita, *The Journal of Physical Chemistry B* **2017**, *121*, 8009-8025; b) B. Ma, R. Nussinov, in *Dynamics in Enzyme Catalysis* (Eds.: J. Klinman, S. Hammes- Schiffer), Springer Berlin Heidelberg, Berlin, Heidelberg, **2013**, pp. 123-137.

[29] C. Aymard, A. Belarbi, *Enzyme Microb. Technol.* **2000**, *27*, 612-618.

[30] E. S. da Silva, V. Gómez-Vallejo, Z. Baz, J. Llop, F. López-Gallego, *Chem. Eur. J.* **2016**, *22*, 13619-13626.

[31] a) S. Velasco-Lozano, E. S. da Silva, J. Llop, F. López-Gallego, *ChemBioChem* **2018**, *19*, 395-403; b) J. M. Bolivar, S. Schelch, T. Mayr, B. Nidetzky, *ACS Catal.* **2015**, *5*, 5984-

5993; c) S. Suárez, C. Guerrero, C. Vera, A. Illanes, *Process Biochem.* **2018**, *73*, 56-64.

[32] S. Rezaei, A. Landarani–Isfahani, M. Moghadam, S. Tangestaninejad, V. Mirkhani, I. Mohammadpoor-Baltork, *Chem. Eng. J.* **2019**, *356*, 423-435.

[33] T. Börner, S. Rämisch, E. R. Reddem, S. Bartsch, A. Vogel, A.-M. W. H. Thunnissen, P. Adlercreutz, C. Grey, *ACS Catal.* **2017**, *7*, 1259-1269.

[34] J. Liu, B. Q. W. Pang, J. P. Adams, R. Snajdrova, Z. Li, *ChemCatChem* **2017**, *9*, 425-431.

[35] Á. Mourelle-Insua, F. S. Aalbers, I. Lavandera, V. Gotor-Fernández, M. W. Fraaije, *Tetrahedron* **2019**, *75*, 1832-1839.

[36] M. D. Jankowski, C. S. Henry, L. J. Broadbelt, V. Hatzimanikatis, *Biophys J* **2008**, *95*, 1487-1499.

[37] a) J. Rocha-Martín, B. L. Rivas, R. Muñoz, J. M. Guisán, F. López-Gallego, *ChemCatChem* **2012**, *4*, 1279-1288; b) X. Ji, Z. Su, P. Wang, G. Ma, S. Zhang, *ACS Nano* **2015**, *9*, 4600-4610; c) D. Valikhani, J. M. Bolivar, A. Dennig, B. Nidetzky, *Biotechnol. Bioeng.* **2018**, *115*, 2416-2425; d) H. A. Reeve, L. Lauterbach, O. Lenz, K. A. Vincent, *ChemCatChem* **2015**, *7*, 3480-3487; e) G. Xu, Y. Jiang, R. Tao, S. Wang, H. Zeng, S. Yang, *Biotechnol. Lett.* **2016**, *38*, 123-129; f) J. Rocha-Martin, A. Acosta, J. M. Guisan, F. Löpez-Gallego, *ChemCatChem* **2015**, *7*, 1939-1947.

[38] a) S.-W. Han, E.-S. Park, J.-Y. Dong, J.-S. Shin, *Appl Environ Microbiol* **2015**, *81*, 6994-7002; b) A. Nobili, F. Steffen-Munsberg, H. Kohls, I. Trentin, C. Schulzke, M. Höhne, U. T. Bornscheuer, *ChemCatChem* **2015**, *7*, 757-760.

[39] J.-D. Zhang, Z.-M. Cui, X.-J. Fan, H.-L. Wu, H.-H. Chang, *Bioproc. Biosyst. Eng.* **2016**, *39*, 603-611.

[40] A. Abdul Halim, N. Szita, F. Baganz, *J. Biotechnol.* **2013**, *168*, 567-575.

[41] C. Nowak, B. Beer, A. Pick, T. Roth, P. Lommes, V. Sieber, *Front. Microbiol.* **2015**, *6*.

[42] J. Sambrook, E. F. Fritsch, T. Maniatis, *Molecular Cloning: A Laboratory Manual*, Cold Spring Harbor Laboratory Press, **1989**.

[43] M. M. Bradford, *Anal Biochem* **1976**, *72*, 248-254.

[44] K. L. Holmes, L. M. Lantz, in *Methods Cell Biol, Vol. 63*, Academic Press, **2001**, pp. 185-204.

[45] S. Bolte, F. P. Cordelieres, *J. Microsc.* **2006**, *224*, 213-232.

[46] J. Wu, M.-H. Li, J.-P. Lin, D.-Z. Wei, *J. Chromatogr. Sci.* **2011**, *49*, 375-378.

13

FULL PAPER

Entry for the Table of Contents

Insert graphic for Table of Contents here.
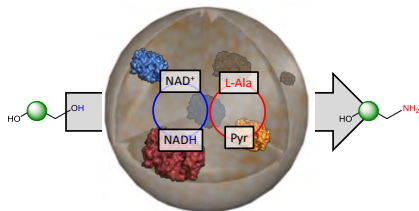
Insert text for Table of Contents here. A multi-enzyme system immobilized on porous agarose beads catalyzed the step-wise synthesis of amino alcohol starting from diols.

Institute and/or researcher Twitter usernames: @HetBiocat and @flopez_gallego